

CHROM. 20 928

ELECTROSORPTIVE DETECTION BASED ON DOUBLE-LAYER CAPACITANCE FOR SELECTED ION MONITORING IN ION CHROMATOGRAPHY

II. SILVER

TORE RAMSTAD and MICHAEL J. WEAVER*

Department of Chemistry, Purdue University, West Lafayette, IN 47907 (U.S.A.)

(First received July 31st, 1987; revised manuscript received August 23rd, 1988)

SUMMARY

A scheme is presented for the detection of selected anions in ion chromatography based on changes in differential double-layer capacitance, ΔC_d , induced by specific anion adsorption on a solid metal electrode. The detector in the liquid chromatography–double-layer capacitance (LC–DLC) arrangement described here is a silver electrode configured in a large-volume wall-jet geometry. The aqueous-phase anions most readily determined by this approach are chloride, bromide, iodide, azide and thiocyanate; additional ions, including iodate, periodate, bromate, thiosulfate and sulfide, are also determinable. Detection limits are sub ppm in most cases. The measurement scheme developed includes provision for faradaic current measurement, thereby providing for simultaneous capacitive and amperometric detection. The benefits of electrode rotation in capacitance detection are also discussed. It is shown that DLC detection is suitable for use with either low-capacity ion chromatography columns or conventional ion exchange columns.

INTRODUCTION

In a previous paper we described the application of differential double-layer capacitance (DLC) detection at mercury – an example of electrosorptive (ES) detection – to the determination of selected anions in ion chromatography (IC)¹. In this technique, based on a.c. impedance measurements, the analyte is detected by means of changes in the differential capacitance, C_d , for an electrode brought about by specific adsorption. Several previous reports have dealt with the coupling of liquid chromatography and electrosorptive detection (LC–ES) for the determination of organic substances on mercury, but our report¹ appears to be the first that treats the determination of ions in an IC mode. Capacitance detection using a solid metal electrode may offer an advantage relative to mercury for the determination of low concentrations of weakly adsorbing ions such as chloride and azide due to the strong adsorption often observed on silver. Another motivation for extending ES detection to a solid electrode is that some analysts find the use of mercury inimical.

Although platinum has been most employed as a solid electrode substrate in fundamental studies², meaningful capacitance measurements cannot be made on this surface for a variety of reasons. Both gold and silver are more suitable substrates and rival each other in terms of the range of anions known to adsorb specifically and in the strength of adsorption³⁻⁶. A dissimilarity between silver and gold, though, is that the potential regions over which adsorption occurs are markedly different, associated with their disparate potentials of zero charge (pzc)³. A potential drawback of gold is that irreversible adsorption effects are often observed⁵, along with capacitance frequency dispersion⁶. Silver does not suffer from these difficulties; overall, it appears to be the "best behaved" of commonly available solid electrode materials. Silver also possesses a wide polarizable potential window, and a proven electrochemical pretreatment procedure is available⁷.

Anions whose adsorption has been studied previously at either single-crystal or polycrystalline silver by means of capacitance measurements include OH^- , ClO_4^- , SO_4^{2-} , Cl^- , Br^- , I^- , N_3^- and SCN^- ^{3,4,8-12}. These studies have shown the last five of these to be strongly adsorbed. Given the desirable characteristics of silver coupled with our previous experience with capacitance measurements at this metal^{8,9}, we undertook a detailed study of the application of silver to DLC detection of anions. (Adsorption of common *cations* is far less pronounced¹³, and hence DLC detection is less applicable to this class of ions). The results of this work are described here. Besides the examination of inorganic anions using DLC at mercury, as already noted¹, we also have reported elsewhere the application of this technique to the detection of simple charged organic species¹⁴.

BACKGROUND

Since a detailed discussion of the principles underlying DLC detection was given in ref. 1, only the salient points will be noted here. Fundamentally, the technique is based on the variations in differential double-layer capacitance, ΔC_d , caused at an electrode poised at a suitable potential by specific adsorption of analyte as it flows past the electrode detector. In contrast to conventional faradaic electrochemical detection, then, this scheme relies on sensing changes in *non-faradaic* currents, most simply obtained from a.c. impedance measurements. Such a detector will provide a reversible response provided that the adsorption-desorption kinetics are suitably rapid.

Of obvious importance is the relationship between the measured ΔC_d values and the analyte concentration, c_x . If the adsorbate surface concentration, Γ_x (mol cm^{-2}), is sufficiently small at a given electrode potential so that Γ_x is proportional to c_x , *i.e.*, Henry's Law applies. As shown in ref. 1, we anticipate that ΔC_d will be approximately proportional to c_x . At higher adsorbate concentrations, the effects of increasing anion-anion repulsion are expected to decrease progressively the ΔC_d - c_x slope so that these plots are generally expected to be non-linear. This behavior was confirmed for a number of anionic adsorbates at mercury¹. Fig. 1. gives an example of such a ΔC_d - c_x plot obtained for bromide adsorbed on polycrystalline silver at -0.90 V, taken from ref. 8. The shape of this plot is typically found for other electrode potentials and adsorbates. While the plot does clearly exhibit non-linearity in the manner anticipated above, it also indicates that approximate concordance to a

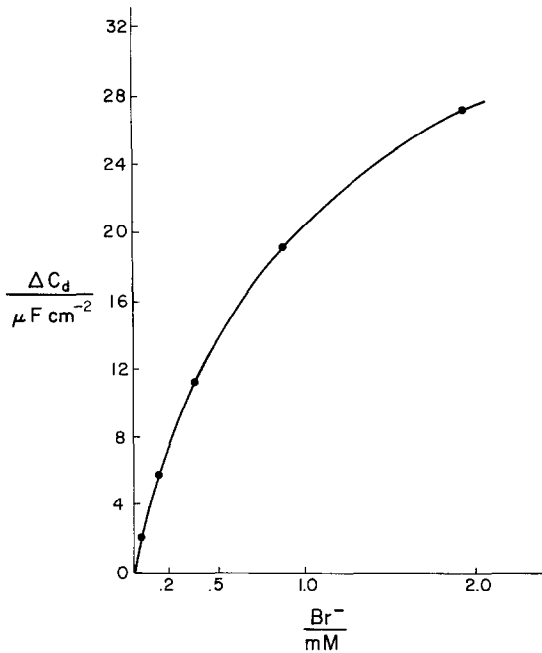


Fig. 1. ΔC_d - c_x curve for Br^- for polycrystalline silver at -0.90 V vs. saturated calomel electrode (SCE); from data given in Fig. 8 of ref. 8. Electrolyte is $(500 - c_x)$ mM sodium fluoride + c_x mM sodium bromide.

linear ΔC_d - c_x relationship can be obtained for relatively small ΔC_d values ($\leq 10 \mu\text{F cm}^{-2}$, *cf.*, ref. 1).

EXPERIMENTAL

Differential double-layer capacitance (DLC) at the silver-aqueous interface was measured using the methodology of phase-sensitive a.c. voltammetry. The instrumental arrangement used is shown in Fig. 2. A 10-mV peak-to-peak sinusoid in the approximate frequency range 50–150 Hz modulates the potential set by a Prince-

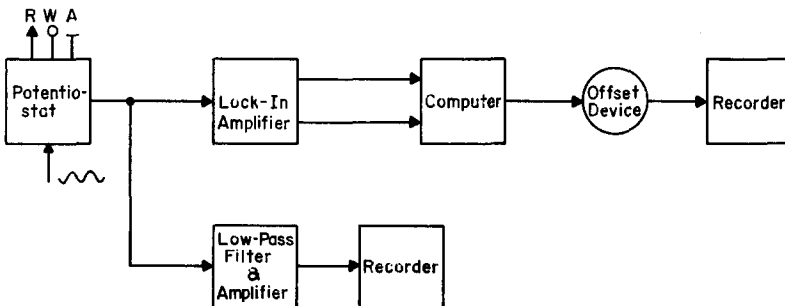


Fig. 2. Block diagram of the instrumental arrangement for the fixed-potential monitoring of differential double-layer capacitance (DLC) at a silver electrode with simultaneous faradaic electrochemical detection. R = Reference electrode; W = working electrode; A = auxiliary electrode.

ton Applied Research Corp. (PAR) 173 or 273 potentiostat. The alternating cell current is separated into its in-phase and out-of-phase components by a PAR 5204 lock-in analyzer. These in turn are directed to a PDP-11/23 computer, which calculates the capacitance according to $C_d = (\omega E)^{-1} [(I_{out}^2 + I_{in}^2) / I_{out}]$, where ω is the frequency in rad s^{-1} , E is the magnitude of the sinusoid and I_{in} and I_{out} are the magnitudes of the in-phase and out-of-phase components, respectively, of the cell current. Changes in the computer output, ΔC_d , are registered by applying the offset output to a strip chart recorder. The low-pass filter/amplifier shown as a parallel branch in Fig. 2 provides for a simultaneous record of the presence of faradaic current. In the event of a sizable faradaic component, the capacitance calculation may be significantly in error. Additional details regarding instrumentation are available elsewhere^{1,15}.

The electrochemical cell used in most experiments is shown in Fig. 3. It is of the large-volume wall-jet type (LVWJ)^{1,16}, its virtues in conjunction with a mercury

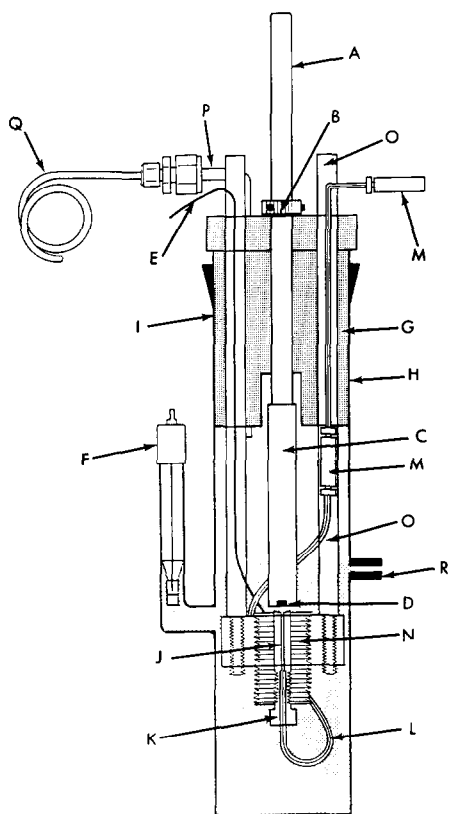


Fig. 3. Large-volume cell with RDE in wall-jet configuration. A = Electrode shank; B = positioning collar; C = PTFE shroud; D = silver working electrode; E = platinum auxiliary electrode; F = silver-silver chloride (3 M sodium chloride) reference electrode; G = PTFE holder; H = cell tube, either 51 or 54 mm; I = 45/50 ground glass joint; J = eluent-delivery capillary (nozzle); K = Upchurch Kel-F male nut; L = 1/16 in. \times 0.3 mm PTFE tubing; M = Swagelok union; N = Kel-F capillary bushing; O = Delrin holder rods for nozzle assembly; P = gas exit tube; Q = capillary pigtail; R = overflow port.

electrode for DLC application are described in ref. 1. An important attribute of the LVWJ design for our application is that virtually any desired supporting electrolyte concentration can be maintained by introducing a high-concentration make-up stream via a port (not shown in Fig. 3). One additional benefit observed for a solid electrode is that when bathed in a non-confining volume, the electrode surface suffers less fouling than when confined to a tiny volume, as in a thin-layer channel. This is an important consideration for a technique whose efficacy depends on the state of the surface. The electrode shown in Fig. 3 is a rotating disk electrode (RDE, Pine Instrument Co.). With this design the electrode can be readily coupled to a rotator, if desired. Our early work on silver, conducted prior to arriving at a final design, made use of a Bioanalytical Systems (BAS) silver detector block (TL-11A cell half), mounted, not in its customary thin-layer configuration, but rather adapted to a wall-jet geometry in the large-volume cell.

Any desired separation between the delivery nozzle and the electrode in Fig. 3 is readily achieved by adjusting the position of the retaining collar (B) on the electrode shank and/or by sliding the eluent capillary delivery assembly up or down via the holder rods (O). When using a rotator (Pine Instrument Co.), additional control is afforded by the rotator height adjustment knob. Use of the rotator required an electrode shank length of ≈ 13 cm, this in addition to a PTFE shroud length of 6.35 cm. The electrode diameter was 2–4 mm, shroud diameters 9–12 mm. A coiled platinum wire served as the auxiliary electrode, and the reference electrode was a BAS silver–silver chloride (3 *M* sodium chloride) Model RE-1 with Vycor membrane.

From an operational standpoint the LVWJ design used here is particularly well suited for rotating an electrode, obviating the problems (engineering, reliability) associated with incorporating an RDE into a miniature (thin-layer) wall-jet design^{17–19}. Rotation of the electrode has a salutary effect on DLC detection in that it sets up a flow steady state. The Schlieren lines, which are otherwise visible in the vicinity of the electrode, vanish as reactants/adsorbates are swept out into solution. The net result is a quieter, straighter C_d -time baseline. A lowered susceptibility to flow variations is a further attribute¹⁷.

Exclusion of oxygen is critical to the performance of silver in DLC detection. A signal arising from the reduction of oxygen can manifest itself in two ways: (1) as a small a.c. component²⁰; and (2) as a larger d.c. signal due to the reduction of oxygen, which can lead to excessive baseline noise. Hence, the entire system – mobile phase reservoir + electrochemical cell – was blanketed under nitrogen. The pigtail shown in Fig. 3. was included to prevent back diffusion of air via the gas exit port.

The silver electrode was mechanically polished, sequentially, with 1.0-, 0.3- and 0.05- μm alumina, either on a wheel or by hand using a specially fabricated PTFE holder; ultrasonication was used to remove residual alumina grit between steps. Mechanical polishing was always followed by an electrochemical polishing sequence⁷. Electrochemical polishing is essential, as without it, both the background capacitance and baseline noise are high and sensitivity (ΔC_d response) prohibitively poor. Subsequent transfer to the working cell was as rapid as possible and was carried out with the working electrode covered with a water meniscus to avoid exposure to air.

All chromatography was conducted with aqueous eluents, prepared in “Milli-Q” water (Millipore). The mobile phase usually consisted of solutions of sodium perchlorate as displacer at concentrations of $2 \cdot 10^{-2}$ *M* and below. Where a higher

concentration of electrolyte was desired, the more weakly displacing NO_3^- was used. Acidic or basic eluents were prepared by adding (usually) perchloric acid or sodium hydroxide, respectively. Similarly to perchlorate²¹, both H^+ and OH^- exhibit negligible or weak specific adsorption at silver²²; this property is desirable for DLC¹.

Prior to introducing column effluent to the cell, the cell was filled with 0.1 *M* sodium perchlorate at an appropriate pH. Throughout an experiment a make-up stream of approximately 0.7 *M* sodium perchlorate was added to the cell at a flow-rate of 0.13 cm³/min in order to maintain an overall cell electrolyte concentration of approximately 0.1 *M*. This is done to offset the dilution that would be caused by continuous delivery of the low-ionic-strength carrier solution; a low overall (sensed) electrolyte concentration leads to increased baseline noise and to consequent higher detection limits. The mobile phase was deoxygenated by nitrogen purging prior to use, and kept under a nitrogen blanket throughout.

A Waters Model 6000A pump was used in conjunction with either a Vydac IC column (silica backbone, No. 302-IC46, The Separations Group), or a Hamilton PRP-X100 IC column (resin based) for most of this work; both columns measured 25 cm long. The guard consisted of Vydac SC pellicular packing with the former and Hamilton PRP-1 with the latter. Receiving less use was a conventional (higher exchange capacity) anion exchange column, a Nucleosil 5SB, also 25 cm long. The injector was a Rheodyne Model 710, usually fitted with a 50- μl loop.

Capacitance-potential (C_a - E) curves were generated in a stationary electrolyte using conventional electrochemical cells for candidate adsorbate ions. These curves allow an assessment of the potential region over which specific adsorption occurs, in order to select suitable conditions at which to conduct the LC-DLC measurements. The curves were obtained using the set-up of Fig. 2 save for the substitution of an X-Y recorder (HP 7045) for the strip chart recorder, and the addition of a ramp driver (PAR 175) to sweep the potentiostat (usually at 5 mV s⁻¹). By keeping the low-pass filter/d.c. amplifier of Fig. 2 in the circuit, the true extent of the polarized window for any analyte could be ascertained simultaneously.

RESULTS AND DISCUSSION

We present here our findings on the utility of electrosorptive detection at silver coupled to ion chromatography. Those anions possessing sufficiently strong adsorptivities to be detectable at analytically useful levels by differential double-layer capacitance are detailed, and their ΔC_a - E and ΔC_a - c_x behavior presented. A discussion is given of the benefits afforded by simultaneous DLC and faradaic electrochemical (FED, amperometric) detection, and of RDE operation. We also describe an extension of DLC detection from low-capacity IC columns to conventional ion exchange columns. All results given pertain to non-stationary, *i.e.*, flowing electrolytes, unless otherwise noted.

Identification of anions suitable for IC-DLC detection

As noted above, many anions specifically adsorb at silver, as at mercury¹. However, we may anticipate that relatively few possess specific adsorbabilities sufficiently large to render them analytically viable in an IC-ES format. We tested virtually all anions of common interest in IC. Of these, five are readily determinable at

concentrations competitive with conductometric detection: Cl^- , N_3^- , Br^- , I^- and SCN^- . Cyanide, which is known to exhibit strong adsorption at silver, presumably did not elute as a sharp band under the chromatographic conditions employed. Several more anions yield "apparent capacitive" responses, which may arise at least partly from anion electroreduction or oxidation. (Note that the capacitance analysis embodied in eqn. 1 is vitiated in the presence of such faradaic processes.) Included among these ions are IO_4^- , IO_3^- , BrO_3^- , S^{2-} and $\text{S}_2\text{O}_3^{2-}$. These ions are further characterized by strong adsorption with, usually, accompanying chromatographic tailing at readily accessible negative potentials. Even if an electrode reaction does occur simultaneously with adsorption, though, there will be virtually no response by a.c. voltammetry if the electrode reaction is irreversible²³, as is the case for these ions, *e.g.*, refs. 24, and 25. Hence, they are also determinable by DLC detection. A further, utilitarian requirement that emerged at silver was that a usable analytical signal manifest itself at a potential no more positive than about -0.5 V: at more positive potentials chromatograms are often subject to baseline disturbances from widespread adsorption. The consequence of this is that surface deactivation can occur quite rapidly.

Plots of relative ΔC_d vs. E are shown for the five adsorptioactive ions listed above in Fig. 4. These curves were obtained by injecting a given concentration of adsorbate into the ion chromatograph over a range of potentials. They can be used to select appropriate potentials for analytical determinations by DLC. An example of a separation obtained for these five ions using specific adsorption detection is given in

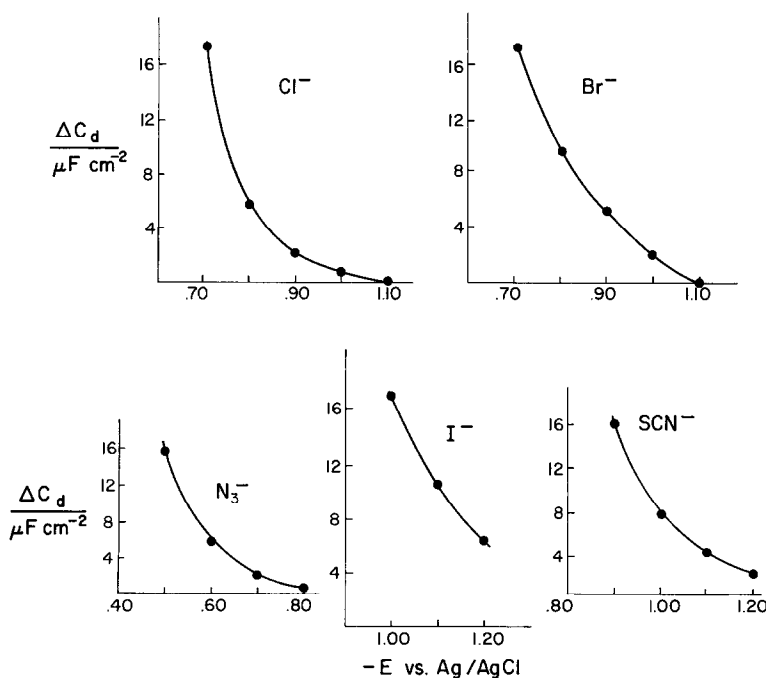


Fig. 4. Relative change in capacitance determined by LC-DLC for five adsorptioactive ions as a function of potential. Concentrations (ppm): Cl^- , 40; Br^- , 10; N_3^- , 50; I^- , 5; SCN^- , 10.

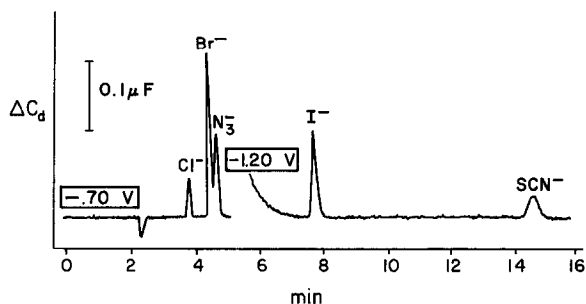


Fig. 5. A separation of five ions with specific adsorption (DLC) detection at silver. Conditions: column, Hamilton PRP-X100; eluent, $1.8 \cdot 10^{-2}$ F sodium perchlorate, pH 10.1 with sodium hydroxide; flow-rate, $0.9\text{ cm}^3/\text{min}$; initially in cell, 0.1 F sodium perchlorate, pH 10.1; make-up, 0.74 F sodium perchlorate, pH 10.1, pumped at $0.13\text{ cm}^3/\text{min}$; sample composition: 20 ppm Cl^- , 5 ppm Br^- , 25 ppm N_3^- , 10 ppm CN^- (not detected), 5 ppm I^- and 25 ppm SCN^- .

Fig. 5. A difference evident here compared to corresponding chromatograms obtained for mercury¹ is the potential region over which specific adsorption occurs; this results from the more negative pzc of silver (*ca.* -0.95 V , ref. 8) relative to mercury (-0.43 V , ref. 26). (These values refer to non-specifically adsorbing electrolytes). Note that two applied potentials (-0.70 and -1.20 V) were used to produce the chromatogram in Fig. 5. Other potentials could be chosen as well. Hence, considerable control over selectivity is available.

Similar to the situation at mercury¹, several of these "cleanly" adsorptioactive anions – Br^- , I^- , SCN^- (plus CN^-) – are also detectable amperometrically at silver, albeit at considerably more positive potentials^{27,28} than those required for specific adsorption detection. Detection limits by amperometry are generally lower, by an order of magnitude²⁹, than those achieved by DLC. However, detection at the more positive potentials required for electrooxidation can lead to irreversible changes in the metal surface. A case in point is provided by the detection of halides, in which the product of the electrochemical reaction is the poorly soluble AgX , where X is a halide. An advantageous feature of the DLC method is that detection occurs at more negative potentials, within the ideally polarized region. A distinct advantage of silver relative to mercury for specific adsorption detection is that all specifically adsorbing anions can be determined at potentials well negative of where metal dissolution occurs.

Detection limits obtained at silver by DCL detection are slightly lower than those obtained at mercury, ≈ 0.2 vs. 0.5 ppm ($50\text{-}\mu\text{l}$ loop). In general, for any concentration of analyte, the signal-to-noise is somewhat superior with silver. Obviously, where lower detection limits are required, either a preconcentration step could be used, preferably on-line and automated³⁰, or larger volumes could be injected^{31,32}. The detection limits realized at silver are comparable to those generally cited $0.2\text{--}1.0\text{ ppm}$ – for both conductometry and indirect photometry³¹, the two most popular forms of detection in IC.

Capacitance–concentration ($\Delta C_d\text{--}c_x$) calibration curves were generated by IC–DLC for Cl^- , N_3^- , Br^- and I^- at silver. The first three were obtained at a stationary electrode (BAS half-cell operated as a wall-jet), the last at an RDE rotated at 400

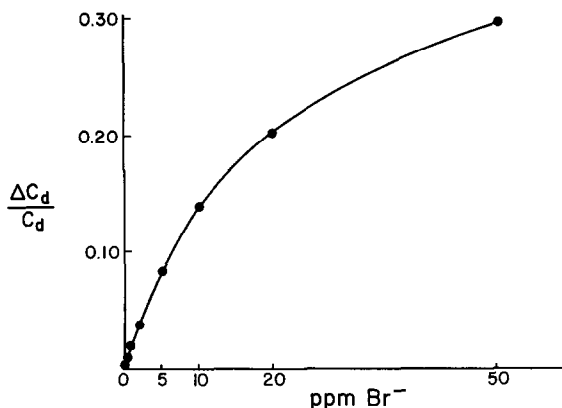


Fig. 6. DLC calibration curve for Br^- at -0.80 V and at a frequency $f = 145$ Hz, obtained using essentially the chromatographic/electrolyte conditions of Fig. 5 save for the substitution of the Vydac column for the Hamilton; 1 ppm Br^- corresponds to $1.25 \cdot 10^{-2}$ mM.

rpm. The curve in Fig. 6, which is a plot of $\Delta C_d/C_d$ vs. concentration of Br^- from the limit of detection, 0.2 ppm ($= 2.5 \cdot 10^{-3}$ mM), to 50 ppm ($= 0.62$ mM) (50- μ l loop), with $E = -0.80$ V, is representative of those obtained. Note that the nature of the response agrees with that expected, *cf.*, Figs. 1 and 6. While the curvature over the tested concentration range is somewhat greater for silver than for mercury¹, the relative change in capacitance is also greater, a reflection of stronger adsorption on silver. Calibration plots for Cl^- and N_3^- at -0.70 V (not shown) show less curvature than that for Br^- at -0.80 V, which is consistent with their lower adsorptivities, whereas at -0.60 V the plot curvature for these two ions is comparable to that for bromide at -0.80 V (Fig. 6). This again is in agreement with the anticipated greater degree of ΔC_d-c_x curvature at more positive potentials since more extensive adsorption, and hence larger ΔC_d values, occur under these conditions. Generally speaking, the closest approach to linearity is observed at more negative potentials. This is exemplified in a plot of $\Delta C_d/C_d$ vs. c_x for I^- at -1.20 V shown in Fig. 7; less curvature

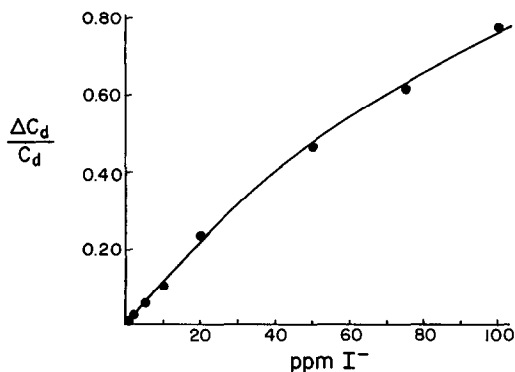


Fig. 7. DLC calibration curve for I^- at -1.20 V and at a frequency $f = 45$ Hz, obtained using the conditions of Fig. 5; 1 ppm I^- corresponds to $7.9 \cdot 10^{-3}$ mM.

is seen in Fig. 7 compared to Fig. 6 even though the former spans a larger range of $\Delta C_d/C_d$ values. It is noteworthy that chromatographic peak tailing was minimal or non-existent for each of these ions at the potentials used in generating the calibration curves. The chloride, azide and bromide experiments employed the Vydac column, using either sodium nitrate or sodium perchlorate as displacer, whereas iodide was examined with the Hamilton PRP-X100 using sodium perchlorate.

Detector optimization

The LVWJ concept has been described in detail^{1,15,16}. A revolutionary aspect of the LVWJ design is that the separation between the effluent delivery nozzle and the working electrode may be varied over a considerable distance, depending on conditions, with no increase in chromatographic band dispersion. Hence, there is no one optimum electrode–nozzle separation. At small separations for the low electrolyte concentrations commonly employed in IC, the in-phase current grows greatly at the expense of the quadrature (out-of-phase) component, *i.e.*, the effective solution resistance increases. This happens because, as the separation becomes smaller, the electrode senses more completely the low-ionic-strength effluent stream and less of the higher-concentration batching solution. The consequence of this is dramatically increased noise, higher detection limits and generally unreliable performance. The maximum allowable electrode–nozzle separation is dictated by the onset of peak broadening, although well before this occurs the response declines to an unacceptably low level. We generally observed best overall performance at a separation of ≈ 1.2 – 1.6 mm.

A potential pitfall attendant to DLC detection at silver is that the ΔC_d response can diminish rapidly with time, presumably due to the accumulation of adsorbed matter. However, this occurrence can be avoided through vigilant attention to detail. The major precaution to be taken is the avoidance of overly positive monitoring potentials. In most instances a suitable compromise between sensitivity and longevity is provided by a potential setting 0.2–0.3 V negative of the maximum in the C_d – E or ΔC_d – E curve. With due care we are able to run for an entire day incurring only minimal losses in sensitivity. However, in the event of reduced response, virtual full restoration of the sensitivity can usually be achieved by stepping to a sufficiently negative potential for a short period. Consequently, an alternate approach is to employ a measurement scheme that incorporates a periodic cleaning pulse. We have devised two: (1) a differential DLC measurement that includes a negative-going desorption step, and (2) a pulse coulometric measurement scheme that utilizes positive-going potential steps from suitably negative values. A detailed description of these two techniques is given in a separate report¹⁴.

Simultaneous faradaic detection and RDE operation

As previously mentioned, the cell/electrode configuration used here made for ready coupling of an RDE to a rotator. As also stated, a rotating electrode has a beneficial effect on DLC detection by creating a steady state flow condition which leads to a straighter baseline. Presumably, by sweeping material away from the electrode and out into solution, the electrode is less susceptible to accumulation of impurities. The net result is that there is less drift in the in-phase and out-of-phase current components. Use of a rotator does not introduce significant noise until a rotation

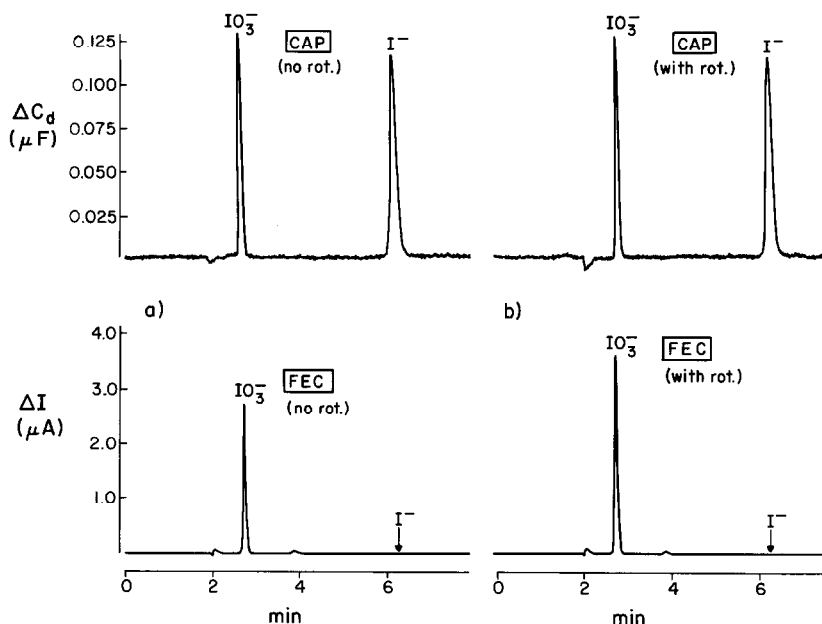


Fig. 8. Demonstration of the utility of electrode rotation in conjunction with combined DLC and FED detection; sinusoidal frequency, $f = 45$ Hz; rotational frequency, ω (a) 0, (b) 2150 rpm; potential, -1.20 V; sample composition: 5 ppm IO_3^- , ≈ 5 ppm I^- .

speed of about 750 rpm is reached. Of course, quite apart from its use in capacitance detection, the cell/electrode/rotator configuration used here is also suitable for faradaic ED (FED) measurements by providing well defined and reproducible mass transport of the electroactive species to and from the electrode surface.

An example of the utility afforded by use of a rotator is evident in Fig. 8 which shows simultaneous DLC and FED chromatograms for IO_3^- and I^- with (a) no electrode rotation, and (b) at a rotation speed of 400 rpm. As expected, the purely capacitive response for I^- is unaffected by rotation, whereas the d.c. FED response for IO_3^- shows the expected effect. As attested to by the invariant "apparent capacitive" response for IO_3^- , its response is also essentially purely capacitive. This is because the reduction of iodate is irreversible²⁴, and hence, virtually no faradaic signal is obtained by a.c. voltammetry²³.

A simultaneous amperometric signal, as obtained above, serves both to complement DLC detection and to act as a sentry toward it. Fig. 8 above provides an example in conjunction with electrode rotation. Another example, but without rotation, is presented in Fig. 9. As seen in Fig. 9a, the DLC response at -1.20 V to $\text{S}_2\text{O}_3^{2-}$ is very weak, but the d.c. faradaic, reductive signal is strong, and *vice versa* for I^- . Hence, one species is detected readily by DLC (I^-) and the other by amperometry ($\text{S}_2\text{O}_3^{2-}$) at this potential. Fig. 9b shows a separation of IO_4^- and I^- . The d.c. response for the reduction of IO_4^- signals an alert that the corresponding "capacitive" trace may not be entirely valid, although again in this case the apparent capacitance is essentially a true value since the reduction of IO_4^- is also irreversible²⁴. Of

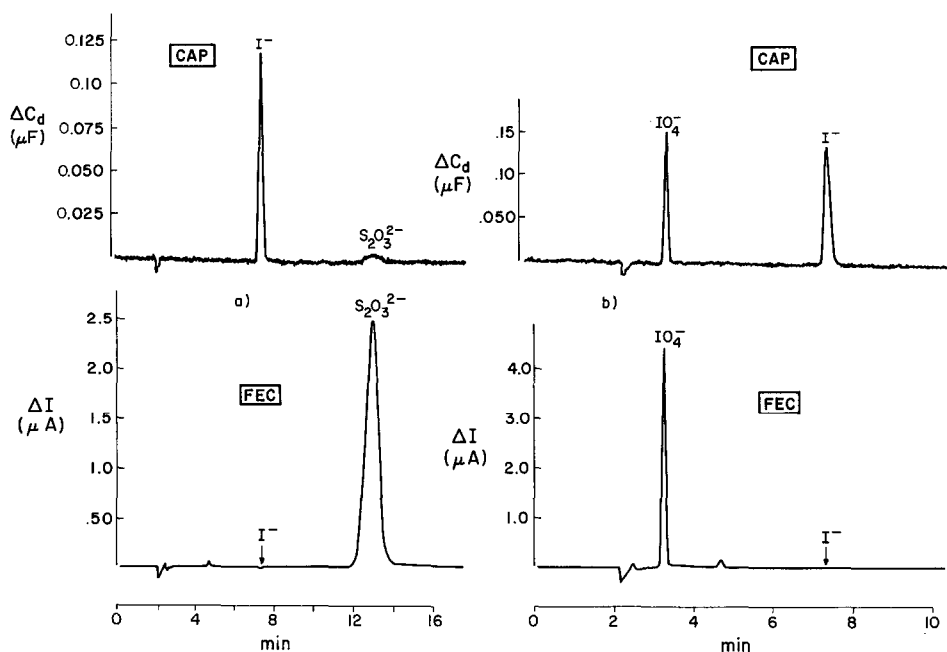


Fig. 9. Dual and FED traces for (a) a 5 ppm I^- /5 ppm $S_2O_3^{2-}$ mixture, and (b) a 10 ppm IO_4^- /5 ppm I^- mixture; both separations conducted with $E = -1.20$ V.

course, with simultaneous amperometric detection, an invalid capacitance output may be viewed as immaterial, since in that case, the FED trace would still furnish the requisite quantitation. The double-layer response to I^- in Fig. 9b is valid, since I^- is electroinactive at -1.20 V.

Extension of DLC detection to conventional ion exchange columns

An inconvenience to the use of standard IC columns in DLC detection is that a make-up stream is required to produce a quiet baseline and reliable operation. The relatively small ion exchange capacities of standard IC columns necessitates the use of displacer ion (electrolyte) concentrations on the order of $(1-2) \cdot 10^{-2}$ M and lower (often just a few millimolar with the lightest loaded packings). Such low electrolyte concentrations mitigate against DLC detection. The problem is illustrated in Fig. 10 in which noise and signal levels are compared under different conditions of operation. Fig. 10a shows the 10-mV peak-to-peak modulating sinewave, $f = 145$ Hz, applied atop the d.c. potential. In Fig. 10b we see the alternating portion of the cell current obtained for quiescent operation (no flow) in the LVWJ cell in 0.1 M electrolyte. Upon introduction of eluent and make-up flow concentrations of $2.5 \cdot 10^{-3}$ and 0.64 M, respectively (the intent being to maintain an overall electrolyte concentration of 0.1 M), the a.c. signal in Fig. 10c was obtained. Under the conditions of c, chromatogram d was obtained for a 10-ppm injection of Cl^- . The same experiment performed in the absence of make-up produced the alternating cell current in e and the chromatogram in f. The deterioration in performance is obvious, the result of a

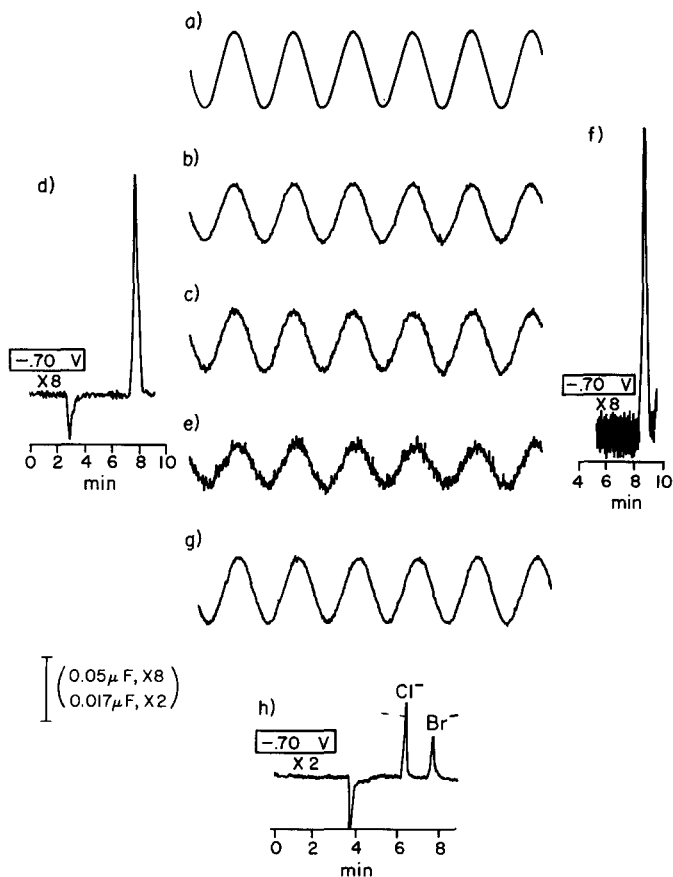


Fig. 10. Comparison of the a.c. current and corresponding chromatograms obtained under varying conditions of operation. See text for details.

substantial solution resistance. Hence, clearly, sensitive capacitance detection under these conditions, *i.e.*, in the absence of make-up is precluded.

Double-layer capacitance detection without a make-up can be achieved, though, by utilizing a conventional anion exchange packing in place of the low-capacity IC packing. This is illustrated in Fig. 10g and h. A Nucleosil 5SB anion exchanger (exchange capacity of 1.0 mequiv./g) with a 0.078 *M* sodium perchlorate eluent (the cell was initially charged with same), produced the a.c. current shown in g and the chromatogram seen in h for an injection of a mixture of 1 ppm Cl^- and 0.5 ppm Br^- . All of the adsorptioactive ions may be similarly determined on the Nucleosil column. While it would be folly to attempt conductometric detection on a conventional ion exchange column, a similar tact has also proven workable in indirect photometric detection^{33,34}.

Operation at higher electrolyte strengths would seem to auger well for double-layer detection using a thin-layer cell, as is commonly used in amperometric detection. Use of a thin-layer device with a low-capacity IC column would require a second

LC pump and post-column addition of a make-up solution. The need for these would be obviated for a thin-layer cell coupled to a high-capacity ion exchange column.

CONCLUSIONS

We have introduced here electrosorption at silver as manifested in changes in double-layer capacitance as a basis of detection in IC. To our knowledge, this is the first application of specific adsorption at a solid electrode to the detection of either inorganic or organic species in liquid chromatography. We have applied the technique at silver to the unequivocal determination of Cl^- , Br^- , N_3^- , I^- and SCN^- at concentrations of interest in contemporary IC. Additional anions, including IO_3^- , IO_4^- , BrO_3^- , S^{2-} and $\text{S}_2\text{O}_3^{2-}$, are also determinable by differential DLC, despite the fact that they undergo electroreduction at the electrosorptive potentials. Presumably, if concentrations higher than those typically determined in modern IC were additionally of interest, the technique could be extended to many other ions.

The $\Delta C_d - c_x$ calibration curves obtained for silver exhibit more non-linearity than those for mercury, but, nevertheless, conform to the shape expected on fundamental grounds. The greater curvature is in part due to stronger adsorption at silver. Detection limits are comparable to those generally claimed for conductivity and indirect photometry, and are marginally better than those achieved using the same procedure at mercury. While some loss of surface activity is unavoidable with time in this technique, careful attention to sample composition/cleanliness and to electrode potential settings allow for extended operation.

ACKNOWLEDGEMENTS

Helpful electronic and computer expertise was generously provided by David Milner. This work has been supported in part by the Office of Naval Research and the Air Force Office of Scientific Research.

REFERENCES

- 1 T. Ramstad and M. J. Weaver, *Anal. Chim. Acta*, 204 (1988) 95.
- 2 P. J. Mitchell, N. A. Hampson and J. S. McNeil, in D. Pletcher (Senior Reporter), *Electrochemistry*, Specialist Periodical Report, Vol. 10, The Royal Society of Chemistry, London, 1985, Ch. 1.
- 3 A. Hamelin, in B. E. Conway, R. E. White and J. O'M. Bockris (Editors), *Modern Aspects of Electrochemistry*, No. 16, Plenum, New York, 1985, Ch. 1.
- 4 W.-kie Paik, M. A. Grenshaw and J. O'M. Bockris, *J. Phys. Chem.*, 74 (1970) 4266.
- 5 A. Hamelin, *J. Electroanal. Chem.*, 142 (1982) 299.
- 6 J. Richer and J. Lipkowski, *J. Electrochem. Soc.*, 131 (1986) 121.
- 7 G. Valette and A. Hamelin, *J. Electroanal. Chem.*, 45 (1973) 301.
- 8 D. Larkin, K. L. Guyer, J. T. Hupp and M. J. Weaver, *J. Electroanal. Chem.*, 138 (1982) 401.
- 9 J. T. Hupp, D. Larkin and M. J. Weaver, *Surf. Sci.*, 125 (1983) 429.
- 10 E. Schmidt and S. Stucki, *Ber. Bunsenges. Phys. Chem.*, 77 (1973) 913.
- 11 M. Fleischmann, J. Robinson and R. Waser, *J. Electroanal. Chem.*, 117 (1981) 257.
- 12 A. V. Shlepakov and E. S. Sevast'yanov, *Sov. Electrochem.*, 14 (1978) 243.
- 13 H. Jehring, *Elektrosorptionsanalyse mit der Wechselstrompolarographie*, Akademie-Verlag, Berlin, 1974, Ch. 2.
- 14 T. Ramstad and M. J. Weaver, *Chromatographia*, 23 (1987) 883.
- 15 T. Ramstad, *Ph. D. Thesis*, Purdue University, 1987, Chs. 2 and 3.

- 16 H. Gunasingham, B. T. Tay and K. P. Ang, *Anal. Chem.*, 56 (1984) 2422.
- 17 A. M. Krstulovic, H. Colin and G. A. Guiochen, *Ad. Chromatogr. (N.Y.)*, (1984) 83.
- 18 W. J. Blaedel and J. Wang, *Anal. Chim. Acta*, 116 (1980) 315.
- 19 B. Oosterhuis, K. Brunt, B. H. C. Westerink and D. A. Doorubos, *Anal. Chem.*, 52 (1980) 203.
- 20 A. M. Bond, *Modern Polarographic Methods in Analytical Chemistry*, Marcel Dekker, New York, 1980, Ch. 7.
- 21 G. Valette, *J. Electroanal. Chem.*, 122 (1981) 295.
- 22 K. L. Guyer, *Ph. D. Thesis*, Michigan State University, 1981, Ch. 3.
- 23 A. M. Bond, *Modern Polarographic Methods in Analytical Chemistry*, Marcel Dekker, New York, 1980, p. 313.
- 24 W. R. Fawcett and Y. C. Kuo Lee, *Can. J. Chem.*, 49 (1971) 2657.
- 25 A. M. Bond, I. D. Heritage, G. G. Wallace and M. J. McCormick, *Anal. Chem.*, 54 (1982) 582.
- 26 D. C. Grahame, *Chem. Rev.*, 41 (1947) 441.
- 27 J. S. Fritz, D. T. Gjerde and C. Pohlandt, *Ion Chromatography*, Hüthig, Heidelberg, 1982, Ch. 3.
- 28 F. C. Smith, Jr. and R. C. Chang, *The Practice of Ion Chromatography*, Wiley, New York, 1983, Ch. 4.
- 29 P. Jandik, D. Cox and D. Wong, *Am. Lab. (Fairfield, Conn.)*, 18(3) (1986) 114.
- 30 A. L. Heckenberg and P. R. Haddad, *J. Chromatogr.*, 350 (1985) 95.
- 31 A. L. Heckenberg and P. R. Haddad, *J. Chromatogr.*, 299 (1984) 301.
- 32 T. Okada and T. Kuwamoto, *J. Chromatogr.*, 350 (1985) 317.
- 33 Z. Iskandarani and T. E. Miller, Jr., *Anal. Chem.*, 57 (1985) 1591.
- 34 P. J. Naish, *Analyst (London)*, 109 (1984) 809.